

# Effects of Poly(vinyl acetate) and Poly(methyl methacrylate) Low-Profile Additives on the Curing of Unsaturated Polyester Resins. II. Morphological Changes During Cure

YAN-JYI HUANG\* and CHIN-CHENG SU

Department of Chemical Engineering, National Taiwan Institute of Technology, Taipei, Taiwan, 107, Republic of China

## SYNOPSIS

The effects of two low-profile additives (LPA), poly(vinyl acetate) (PVAc) and poly(methyl methacrylate) (PMMA), on the morphological changes during the cure of unsaturated polyester (UP) resins at 110°C were investigated by an approach of integrated reaction kinetics-morphology-phase separation measurements by using a differential scanning calorimeter (DSC), scanning electron microscopy (SEM), optical microscopy (OM), and a low-angle laser light-scattering apparatus (LALLS). For the UP resins cured at 110°C, adding LPA could facilitate the phase separation between LPA and crosslinked UP phases early in the reaction, and discrete microgel particles were thus allowed to be identified throughout the reaction. Microvoids and microcracks responsible for the volume shrinkage control could also be observed evidently at the later stage of reaction under SEM. Depending on the types of LPA and the initial molar ratios of styrene to polyester C=C bonds, the morphological changes during the cure varied considerably. The progress of microstructure formation during reaction has been presented. Static ternary phase characteristics for the styrene-UP-LPA system at 25°C have also been employed to elucidate the resulting morphology during the cure in both the continuous and the dispersed phases. © 1995 John Wiley & Sons, Inc.

## INTRODUCTION

In recent years, studies on the effect of low-profile additives (LPA) on the morphology by scanning electron microscopy (SEM) in the cure of unsaturated polyester (UP) resins have been carried out.<sup>1-11</sup> However, most of them were aimed at the ultimately cured products,<sup>1-7,9-10</sup> which pertained to the product- or application-oriented type of research. Although these researchers could not provide clear pictures at high magnification characterized by SEM regarding the morphological changes throughout the reaction caused by LPA, yet Pattison et al.<sup>2,4</sup> and Suspene et al.<sup>9</sup> have also observed the morphological changes in the course of UP curing by using optical microscopy (OM) and have achieved some degrees

of success in elucidation of the LPA mechanism. On the other hand, most recent research by Hsu and Lee<sup>8</sup> and Hsu et al.<sup>11</sup> has been directed toward the morphological changes by SEM for some partially cured samples in the cure of low-shrink UP resins but mainly limited to those samples near the gelation point as well as the ultimately cured samples.

In Part I of this series,<sup>12</sup> the effects of two LPA, poly(vinyl acetate) (PVAc) and poly(methyl methacrylate) (PMMA), on the curing kinetics during the cure of UP resins at 110°C were investigated by using a differential scanning calorimeter (DSC) and a Fourier transform infrared spectrometer (FTIR). In this work, an integrated reaction kinetics-morphology-phase separation measurement was carried out for the low-shrink UP resins at various molar ratios of styrene to polyester C=C bonds by DSC, SEM, OM, and low-angle laser light-scattering (LALLS). The effects of PVAc and PMMA LPAs on the microstructure formation and phase separation during the entire reaction are discussed.

\* To whom correspondence should be addressed.

## EXPERIMENTAL

### Materials

The UP resin ( $\bar{M}_n = 2140$  g/mol, and with 7.72 calculated number of C=C bonds in each polyester molecule) and two LPAs including PVAc (LP40A, Union Carbide,  $\bar{M}_n = 42,000$ ) and PMMA ( $\bar{M}_n = 34,000$ ) used in this study were the same as those in Part I of this series,<sup>12</sup> where detailed characterization of the materials could be found. For the sample solution with LPA, 10% by weight of LPA was added, while the molar ratio of styrene (ST) to polyester C=C bonds was adjusted to be MR = 1/1, 2/1, 3/1 or 6/1. The reaction was initiated by 1% by weight of *tert*-butyl perbenzoate (TBPB) at 110°C. All the materials were employed as received without further purification.

### Instrumentation and Procedure

#### Differential Scanning Calorimetry

The reaction kinetics were measured by a DuPont 9000 differential scanning calorimeter with a 910 pressurized DSC cell at atmospheric pressure. All the reactions were conducted in hermetic aluminum sample pans with sample weights ranging from 6 to 10 mg. Isothermal reaction rate vs. time profiles were measured at 110°C. The method of approach for obtaining the rate of overall reaction and total conversion at a given time during the entire reaction has been described in Part I of this series.<sup>12</sup>

#### Morphology

In the morphological study, the reaction of resin with LPA cured in the DSC cell was stopped at a preset time by rapidly chilling the sample pan in liquid nitrogen for 5 min. The sample was then broken into several pieces and dissolved in dichloromethane for one day to remove all soluble materials. The undissolved sample was placed on a filter paper and dried at room temperature for one day. The dry sample was then gold-coated for morphological measurement. Hitachi S-520 and S-550 scanning electron microscopes with accelerating voltages of 15 and 20 kV were used to observe the fractured surface of each sample at magnifications of 500 $\times$  to 5000 $\times$ .

#### Phase Separation

The phase separation during reaction was followed by a home-made LALLS apparatus, which included mainly a 0.5-mW He-Ne laser source, an unbiased photovoltaic detector, a photodiode readout, and a recorder (Oriel). As suggested by Suspene et al.,<sup>9</sup> the

detecting angle was fixed at 10–20° for measuring microdomains  $> 0.1 \mu\text{m}$ . For a miscible system, the measuring of light scattering would be essentially zero. When microdomains  $> 0.1 \mu\text{m}$  are generated during reaction due to phase separation, the incident laser light would be scattered when emerging from the sample, and the measured light-scattering intensity would be a function of the concentration of microdomains. Due to the sensitivity of laser light scattering, the measurement was carried out in a darkroom.

Prior to the measurement, one drop of sample solution about 0.8 mg was placed between two microscope cover glasses, which were then inserted into a hot stage (Mettler, FP82HT). The phase separation during reaction for the thin layer of sample was detected isothermally at 110°C by following the scattered light intensity vs. time profile. The reaction of resin with LPA cured at 110°C in the hot stage was also stopped at a preset time by rapidly chilling the sample sandwiched between microscope cover glasses in liquid nitrogen. A series of samples with differing degrees of scattering propensity during the entire cure were observed at room temperature under an optical microscope using transmitted light at magnifications of 100 $\times$  to 400 $\times$ .

## RESULTS

#### Effects of LPAs on Morphology

For the neat UP resin at MR = 2/1, SEM micrographs of partially cured samples by using DSC at 110°C have been presented in our previous study.<sup>13</sup> With the addition of LPA, the morphology of the ST-UP-LPA system during the cure was changed dramatically, as shown below, where all of the morphology studies were conducted on DSC specimens. It should be noted that for the morphologies found in the fractured surface of DSC specimens cured *in situ*, they reflected the microstructure buildup that was undissolved by the solvent up to a certain monomer conversion. Although the sample had lost some of its mass in the solvent treatment procedure before being examined in the SEM, the true morphology in the polymerizing blend at the time of cessation of cure could still be revealed or inferred from the observed morphology under SEM. This is because the characteristics of established microstructure for the partially cured sample would not be affected much by the solvent extraction procedure.

#### ST-UP-PVAc System

Figure 1 shows the SEM micrographs of partially cured samples at MR = 2/1 with 10% PVAc. Figure

1(a) was at a conversion of 1.2%. At magnification of 1000 $\times$ , it appeared as a nonuniform, soft, and fluidlike gel, with many small globules distributed throughout the sample surface. On close examination, the globules, about 0.5–1.0  $\mu\text{m}$  in diameter, were seen to be fused together at local spots and tended to form a loose network structure. Figure 1(b) was at a conversion of 4.3%, and a multitude of globules, still about 0.5–1.0  $\mu\text{m}$  in diameter, began to be clearly precipitated from the unreacted resin matrix. Despite some independence associated with these slightly compact globules, they were more or less fused together at such an extent of conversion. As the reaction progressed, more and more globules were generated, kept on phase separating from the matrix, and slightly grew up. At around the maximum point in the DSC rate profile as shown in Figure 1(c) ( $\alpha = 32.6\%$ ), clearly identified and highly independent globules were seen to be closely overlapped with each other, the maximum diameter of which was increased up to 1.5  $\mu\text{m}$ .

After the peak of the DSC rate profile, the formation of globules persisted at a slower pace, and more highly packed globule structures were observed as shown in Figure 1(d) ( $\alpha = 53.4\%$ ). For the final cured sample ( $\alpha = 73.9\%$ ), Figure 1(e) indicates that the globules were intimately overlapped so that most of the voids between them, as seen evidently in the previous sample, were reduced both in number and in size. The maximum diameter of the globule could increase up to 1.8  $\mu\text{m}$  due to a higher monomer conversion. Figure 1(f) shows the SEM micrograph for the same final cured sample as in Figure 1(e), but with no extraction treatment for the fractured surface. The spherical outline of the globule was not as clear as that in Figure 1(e) since its surface was covered by a smooth coating, which was identified as LPA (i.e., PVAc in this case) by Pattison et al.<sup>4</sup> Microvoids ranging from 0.2 to 2  $\mu\text{m}$  in diameter could be observed in the PVAc phase.

Now that the PVAc layer surrounding the globules would be easily washed off in the extraction procedure, for the ST-UP-PVAc reaction system, the series of SEM micrographs shown above suggests that a co-continuous phase consisting of the cross-linked UP (i.e., globules) and PVAc phases would result early in the reaction when a large quantity of globules could phase separate from the matrix.

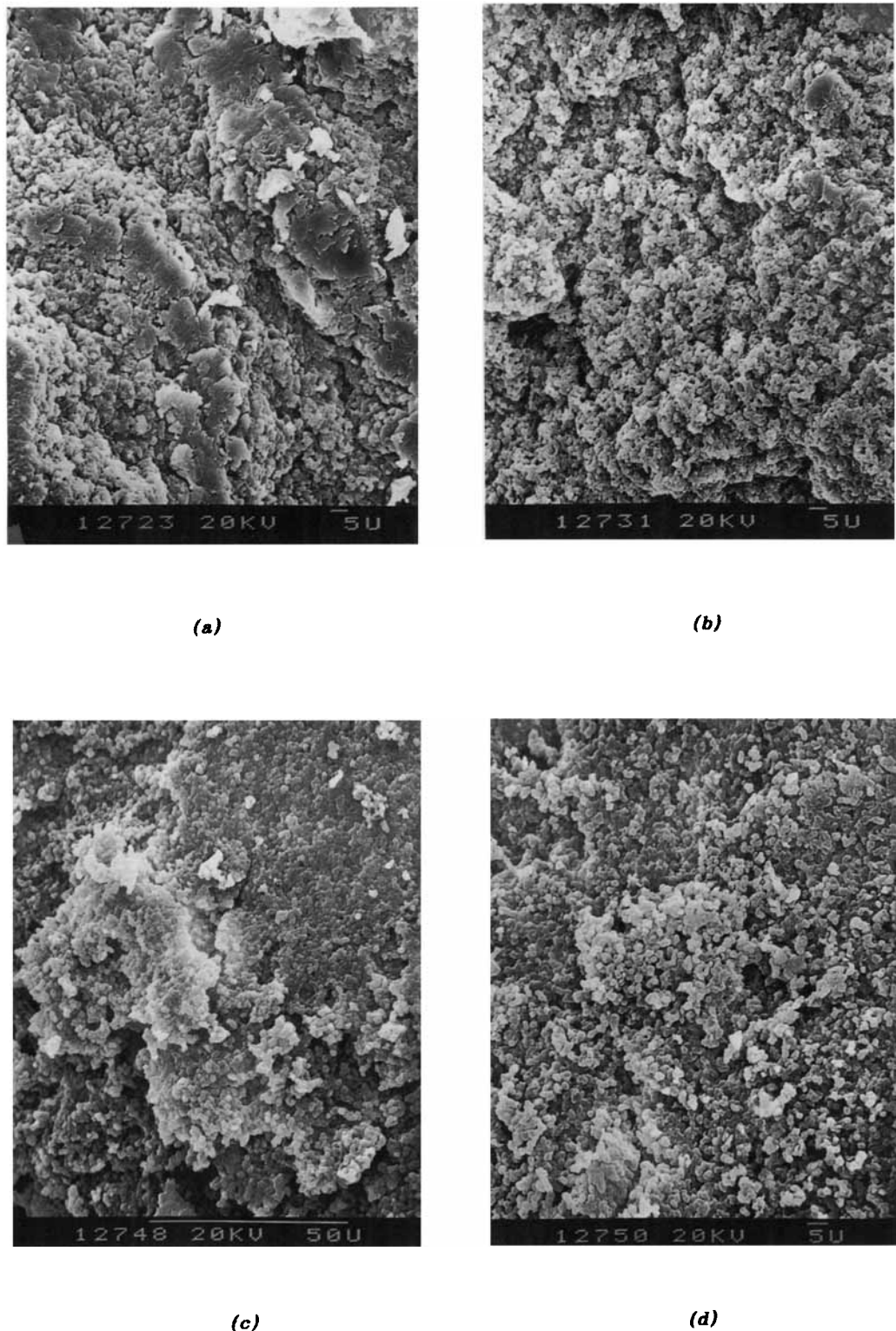
#### Styrene-UP-PMMA System

Figure 2 shows the SEM micrographs of partially cured samples for the UP resins at MR = 2/1 with 10% PMMA. Figure 2(a) ( $\alpha = 0.36\%$ ) indicates a

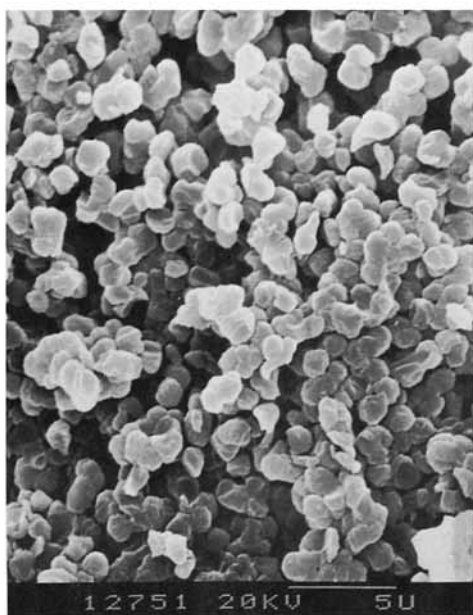
soft gel-like microstructure with many nonuniform holes ranging from 0.1 to 2.5  $\mu\text{m}$  distributed at local spots, which would be due to soluble materials in the PMMA-dispersed phase being extracted by dichloromethane in the preparation of SEM samples. Figure 2(b) ( $\alpha = 0.71\%$ ) shows that at magnification of 1000 $\times$ , the continuous phase formed a loose network all over the sample surface, while the holes left by the PMMA-dispersed phase turned out to be increased in number and were shallow when compared with those in Figure 2(a). At magnification of 5000 $\times$ , globules were formed at some local spots and they tended to be fused together, indicating that cross-linking reactions between styrene and polyester C=C bonds, which were dissolved in the PMMA-dispersed phase, had occurred. As the reaction conversion increased to 4.1% as shown in Figure 2(c), the microstructure of the continuous phase tended to be slightly compact, and appeared flakelike as a whole, where the complex "river markings" were caused by crack plane jumping during fracture, and with many small holes scattered around. In contrast, more and more clearly identified globules with an average diameter of about 1  $\mu\text{m}$  were generated in the PMMA-dispersed phase. It is worthwhile to mention that although the microstructure full of globules in the PMMA-dispersed phase resembled that in Figure 1(b) for the PVAc-containing sample cured to a similar conversion level, the concentration of globules appeared much lower for the former than for the latter.

As the reaction proceeded, the flakelike microstructure in the continuous phase became even more compact. Meanwhile, the number of globules generated in the PMMA-dispersed phase was enhanced and they were closely overlapped with each other. Moreover, the size distribution of the globules turned out to be nonuniform, as shown in Figures 2(d) ( $\alpha = 33.4\%$ ) and 2(e) ( $\alpha = 48.6\%$ ), which would be due to the less compatibility between PMMA and UP resins. Figure 2(d), corresponding to around the maximum point in the DSC rate profile, shows that the globule size in the PMMA-dispersed phase mostly ranged from 0.5 to 1.5  $\mu\text{m}$ . At such a conversion level, when compared with the PVAc-containing sample shown in Figure 1(c), the globules in the PMMA-dispersed phase here appeared nonuniform in size, less independent of neighboring globules, and less clear in their spherical outlines.

Figure 2(f) shows the final cured sample with a conversion of 77.3%. It clearly indicates that in the PMMA-dispersed phase the number of large globules (1.5–2  $\mu\text{m}$ ) increased somewhat, whereas the number of small globules (< 0.1  $\mu\text{m}$ ) was greatly

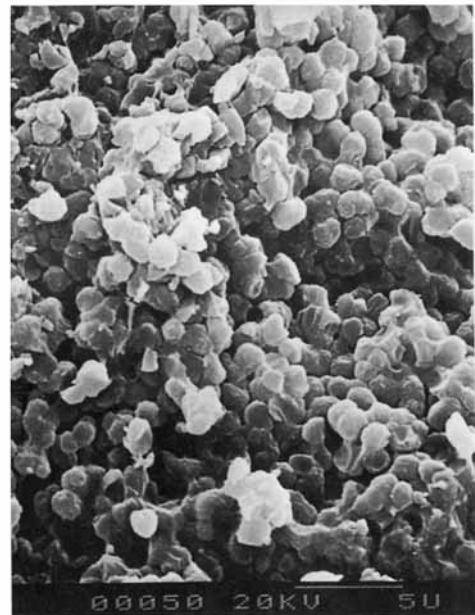


**Figure 1** SEM micrographs of the fractured surface for UP samples with  $MR = 2/1$  and 10% PVAc cured isothermally at  $110^\circ\text{C}$  to various conversion levels. (a)  $\alpha = 1.2\%$ , (b)  $\alpha = 4.3\%$ , (c)  $\alpha = 32.6\%$ , (d)  $\alpha = 53.4\%$ , (e)  $\alpha = 73.9\%$ , and (f)  $\alpha = 73.9\%$  but with no extraction treatment for the fractured surface. Pictures (a)–(c) magnify at  $1000\times$ , (d)–(e) at  $1000\times$  and  $5000\times$ , and (f) at  $5000\times$ .



(d')

(e)



(e')

(f)

**Figure 1** (Continued from the previous page)

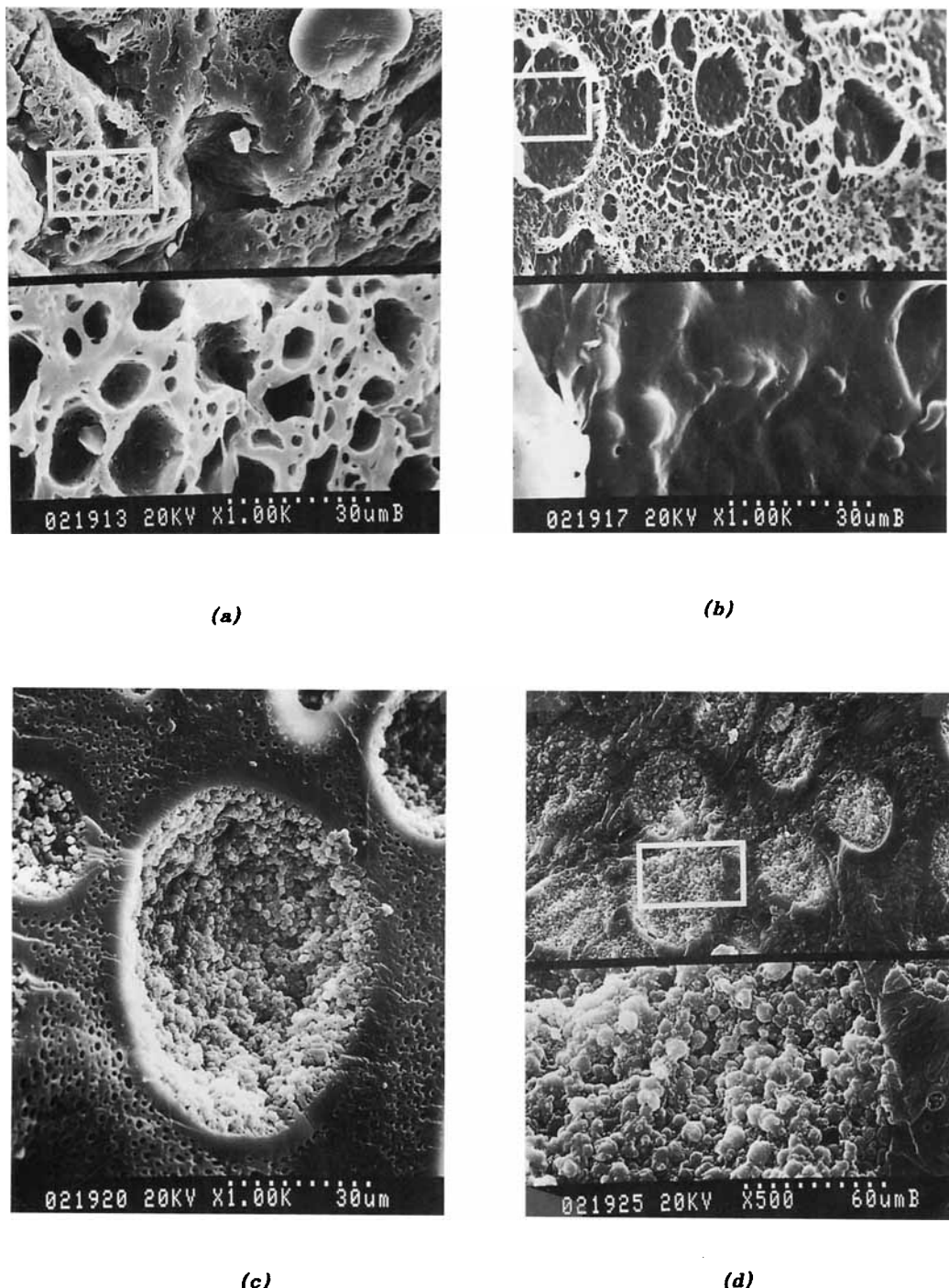


**Figure 2** SEM micrographs of the fractured surface for UP samples with  $MR = 2/1$  and 10% PMMA cured isothermally at  $110^\circ\text{C}$  to various conversion levels. (a)  $\alpha = 0.36\%$ , (b)  $\alpha = 0.71\%$ , (c)  $\alpha = 4.1\%$ , (d)  $\alpha = 33.4\%$ , (e)  $\alpha = 48.6\%$ , (f)  $\alpha = 77.3\%$ , and (g)  $\alpha = 77.3\%$  but with no extraction treatment for the fractured surface. The upper picture magnifies at  $500\times$  or  $1000\times$ , and the lower one for the upper designated region at  $2500\times$  or  $5000\times$ ; (c) and (f') magnify at  $1000\times$ .

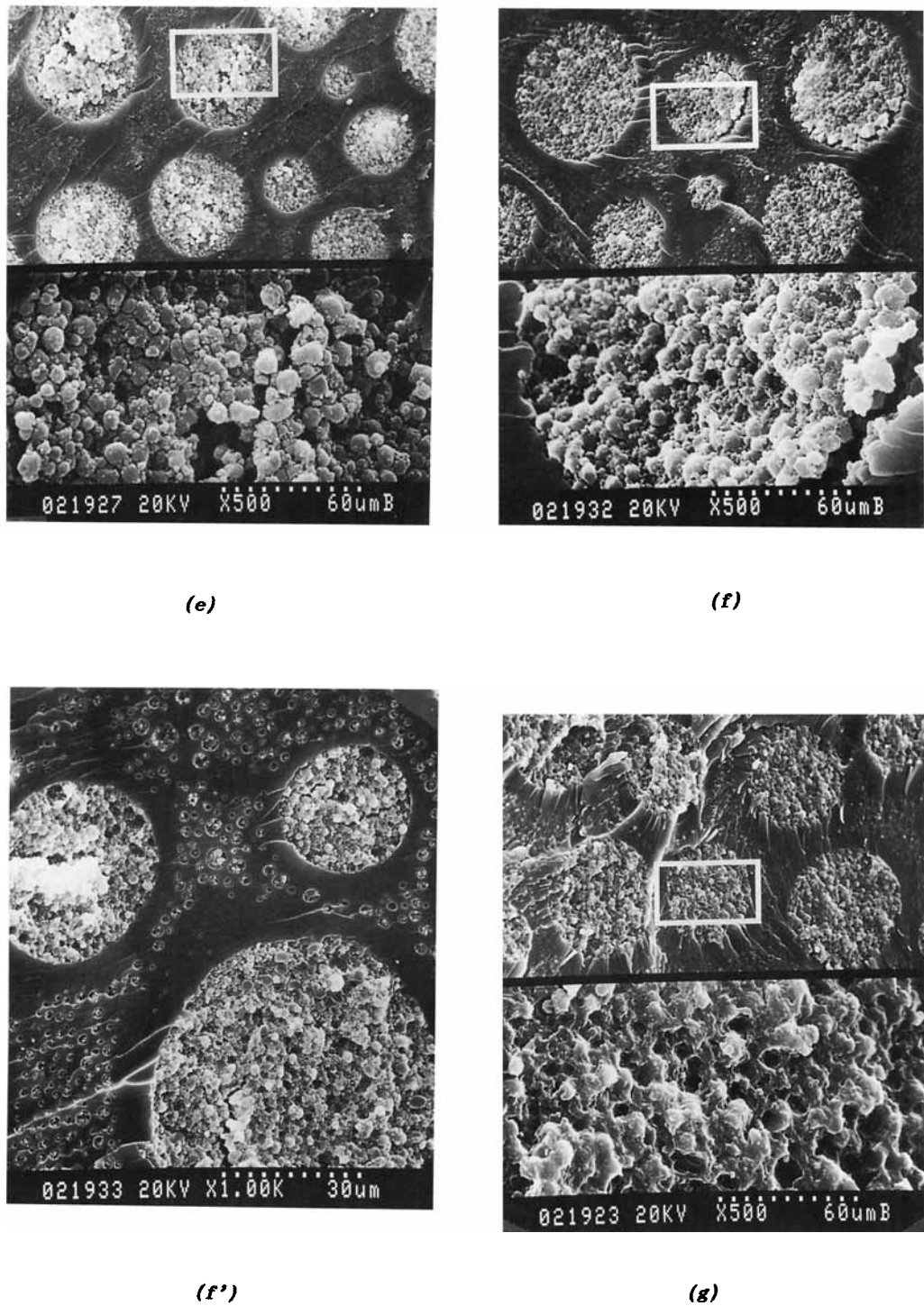


Figure 2 (Continued from the previous page)

elevated. At magnification of 1000 $\times$ , small globules ( $<0.1\text{ }\mu\text{m}$ ) could also be observed inside the small PMMA-dispersed phase that was scattered around the continuous phase. At magnification of 500 $\times$  or 2500 $\times$ , microcracks (1–2  $\mu\text{m}$  wide) along the inter-

face between the crosslinked UP continuous phase and the PMMA-dispersed phase and microvoids inside the PMMA-dispersed phase emerged, both of which could also be identified inside the PMMA-dispersed phase as shown at magnification of 1000 $\times$ .

It should be noted that it was at the later stages of cure (i.e., after the peak of DSC rate profile) that an LPA-depleted zone (i.e., microvoids) developed around some of the globules in the PMMA-dispersed phase [see Figs. 2(d)–(f)].

Figure 2(g) shows the same final cured sample as that in Figure 2(f), but with no solvent treatment for the fractured surface. The globules in the PMMA-dispersed phase was covered by a thin coating, which was identified as LPA<sup>2</sup> (i.e., PMMA in this case). The continuous phase also seemed to be coated by a layer of PMMA [compare Figs. 2(f) and 2(g)]. Therefore, the PMMA-dispersed phase would be actually comprised of the crosslinked UP phase (i.e., globules) and the PMMA phase, which took some resemblance to a co-continuous phase structure mentioned earlier for the PVAc-containing sample. At magnification of 2500 $\times$ , a number of microvoids, 0.5–2.0  $\mu\text{m}$  in diameter, around the globules could be observed in the PMMA-dispersed phase.

### Effects of Comonomer Compositions on Morphology

In order to investigate the effects of molar ratios of styrene to polyester C=C bonds (i.e., comonomer compositions) on the morphology during curing, SEM micrographs of partially cured samples at 110°C by using DSC were also obtained for the PVAc-containing and the PMMA-containing samples at MR = 1/1, 3/1, and 6/1.

### ST-UP-PVAc System

For MR = 1/1, 3/1, and 6/1, the globule microstructure characteristics for the UP resins with 10% PVAc during the cure were essentially similar to that for MR = 2/1. However, there were several salient distinctions in morphology due to the varied styrene content among the reaction systems.

At very low conversions (1–5%), the microstructure was soft and fluidlike (see Fig. 3). At MR = 1/1, a webbed microstructure through connecting soft globules could be observed evidently. As the molar ratio increased to MR = 3/1, the overall microstructure exhibited a loose gel and no globules could be easily identified. Further increasing the molar ratio to MR = 6/1 resulted in a more slack microstructure than that of MR = 3/1.

At a conversion of 5–10%, a number of distinguishable globules were generated and overlapped with each other (see Fig. 4). At MR = 1/1, the individual globule appeared slightly compact, marked in its spherical boundary and less fused with neighbor-

boring ones. As the molar ratio increased, the globules tended to be fused together to a greater extent and less clear in their spherical shapes.

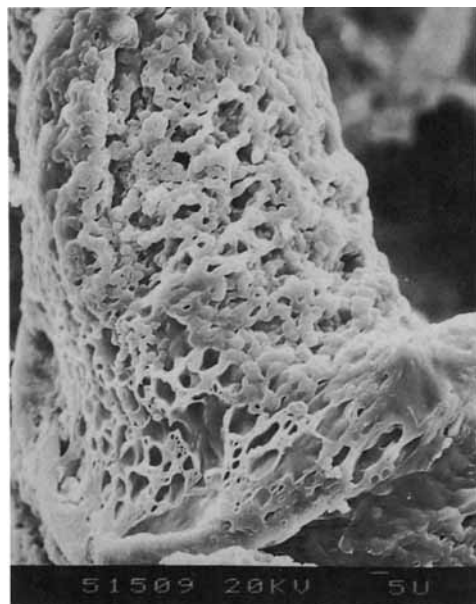
At high conversions (70–90%), a great number of globules were intimately packed together, which was similar to that in Figure 1(e). However, the SEM micrographs (not shown) indicate that as the molar ratio increased, the globules appeared much greater in number, more packed, less spherical in shape, and tended to appreciably connect with neighboring ones throughout the sample surface. Also, the average size of the globule at MR = 6/1 was apparently smaller than that at MR = 1/1 and 3/1 (1.5 vs. 2.0  $\mu\text{m}$ ).

### ST-UP-PMMA System

For MR = 1/1, 3/1, and 6/1, the microstructure for the UP resins with 10% PMMA in the cure exhibited a two-phase feature similar to that of MR = 2/1. However, depending on the initial molar ratio of styrene to polyester C=C bonds, varied phase characteristics would result. The overall morphology with a globule microstructure in the PMMA-dispersed phase and a flakelike microstructure in the crosslinked UP continuous phase as seen at MR = 2/1 could not be retained at some other molar ratios. The progress of microstructure formation during different stages of reaction conversions at MR = 1/1, 3/1, and 6/1 will be described below in elucidation of the resulting morphology for the final cured samples.

At a conversion of 1–5%, the microstructure was more or less viscous fluidlike, and the local microgel structures were loosely linked to span over the system (see Fig. 5). At MR = 1/1, no globules could be identified. As the molar ratio increased, the soft globules generated became more clearly identified and less fused with each other.

At a conversion of 11–15%, either the continuous or the dispersed phase exhibited globule microstructure with differing degrees of clarity and size uniformity (see Fig. 6). At MR = 1/1, the phase separation phenomenon occurred. In both phases, many vague globules appeared closely overlapped so that very rough and flakelike surfaces resulted. At MR = 3/1, only single phase composed of a number of globules with a nonuniform size distribution could be observed. Most of the globules possessed a diameter of 0.5–5  $\mu\text{m}$ , while the diameter of some large ones that were scattered around could be as large as 25–40  $\mu\text{m}$ . At MR = 6/1, both the continuous and PMMA-dispersed phases contained a great number of globules (1.5–2.0  $\mu\text{m}$  in diameter). Some materials



(a)

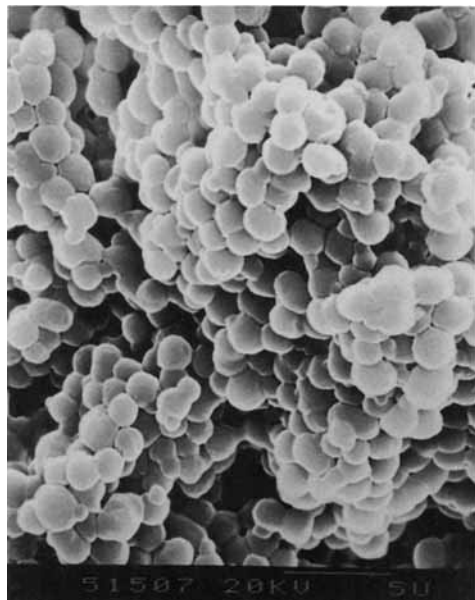


(b)

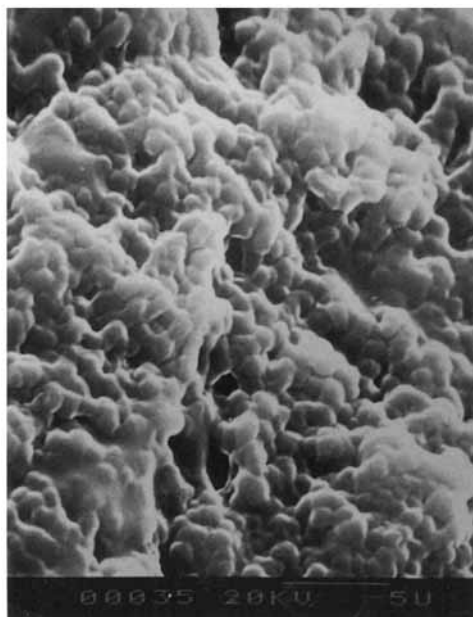


(c)

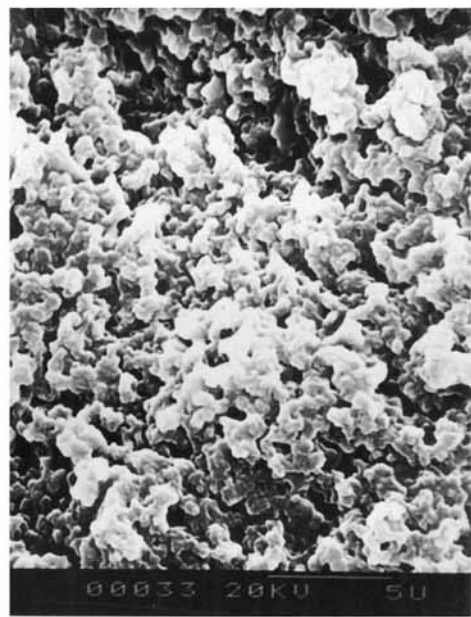
**Figure 3** SEM micrographs of the fractured surface at 1000 $\times$  for the 10% PVAc-containing samples at various molar ratios cured isothermally at 110°C to 1–5% conversion. (a) MR = 1/1,  $\alpha$  = 1.0%; (b) MR = 3/1,  $\alpha$  = 2.2%; and (c) MR = 6/1,  $\alpha$  = 4.6%.



(a)



(b)

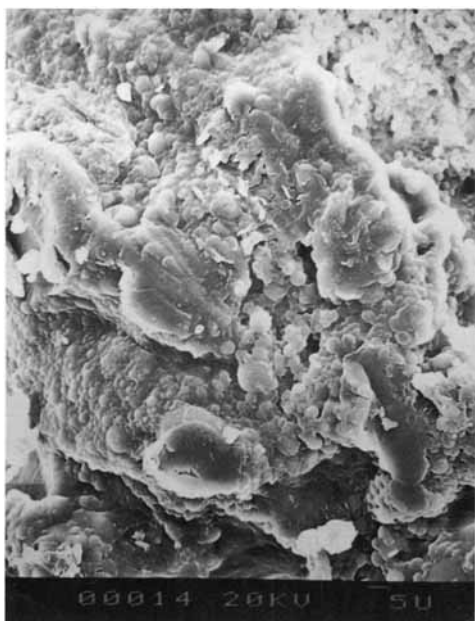


(c)

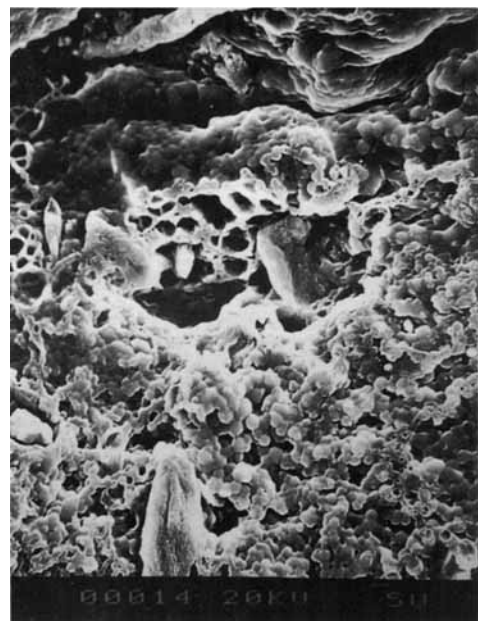
**Figure 4** SEM micrographs of the fractured surface at 5000 $\times$  for the 10% PVAc-containing samples at various molar ratios cured isothermally at 110°C to 5–10% conversion. (a) MR = 1/1,  $\alpha$  = 6.9%; (b) MR = 3/1,  $\alpha$  = 4.0%; and (c) MR = 6/1,  $\alpha$  = 7.1%.



(a)



(b)



(c)

**Figure 5** SEM micrographs of the fractured surface at 1000 $\times$  for the 10% PMMA-containing samples at various molar ratios cured isothermally at 110°C to 1–5% conversion. (a) MR = 1/1,  $\alpha$  = 1.9%; (b) MR = 3/1,  $\alpha$  = 3.7%; and (c) MR = 6/1,  $\alpha$  = 3.1%.

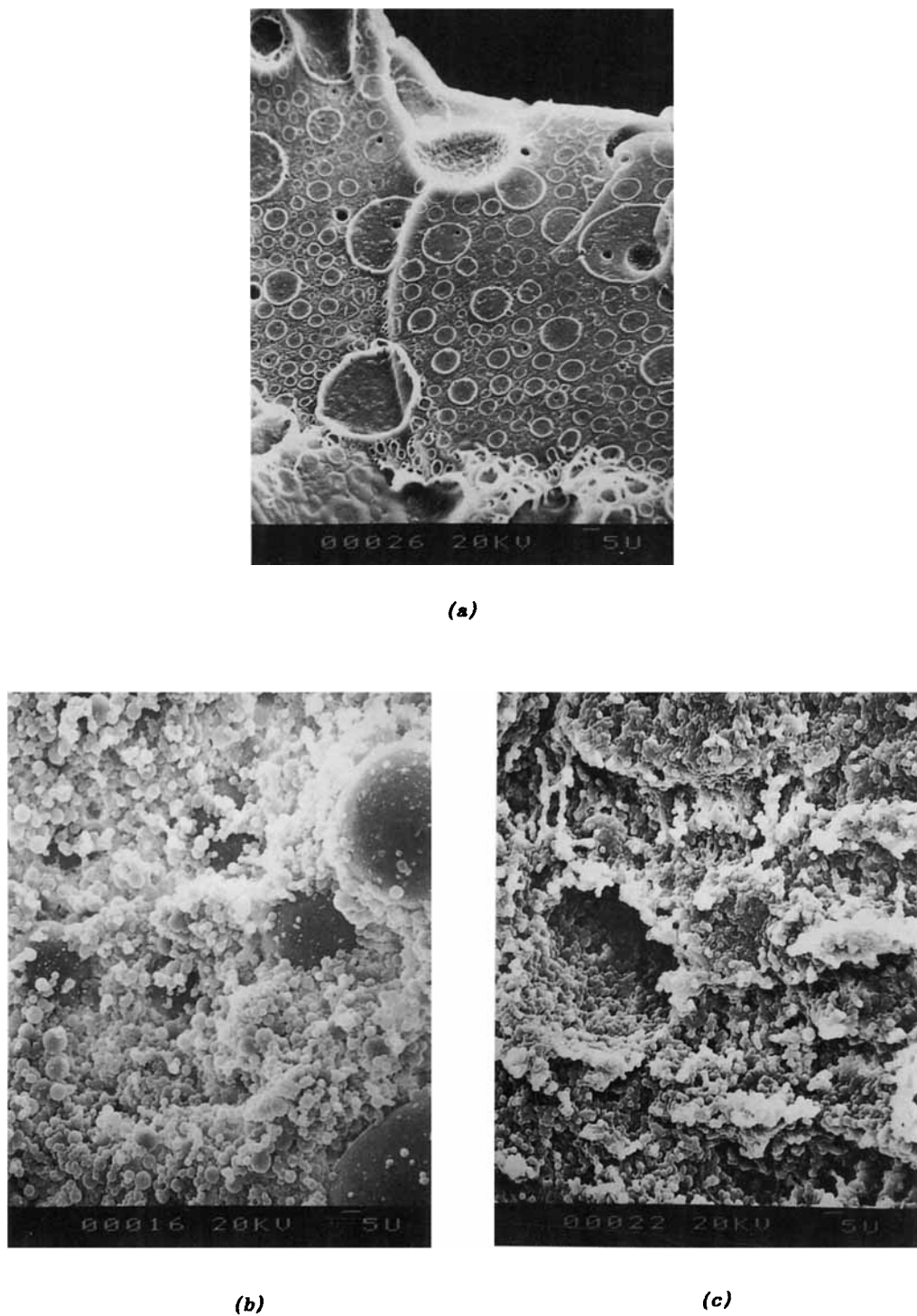


**Figure 6** SEM micrographs of the fractured surface at 1000X for the 10% PMMA-containing samples at various molar ratios cured isothermally at 110°C to 11–15% conversion. (a)  $MR = 1/1$ ,  $\alpha = 12.1\%$ ; (b)  $MR = 3/1$ ,  $\alpha = 12.1\%$ ; and (c)  $MR = 6/1$ ,  $\alpha = 13.8\%$ .

with yellow index values rising up to 18 for the 2 mm-thick intercalate.

A significant improvement was achieved by using BuA as the reactive diluent, in association with AA (formulations **8–14**). The cure speed was markedly increased, while at the same time a highly transparent noncolored polymer was formed that showed good adhesion to glass and excellent impact resistance. The AA content had to be maintained to at least 10% in order to ensure high adhesion to glass and cohesive fracture upon impact. The AA can be partly or totally replaced by methacrylic acid (formulation **12**), without significant changes in the laminate characteristics, except for the expected decrease in the resin reactivity. The best overall performance was achieved with a resin containing 65% Actilane 9, 25% BuA, and 10% AA (formulation **13**). This glass laminate was found to withstand, without breaking, 10 consecutive impacts of a 400 g steel bead dropped from an height of 3 m. The addition of small amounts (5%) of a polyester hexaacrylate (Ebecryl 830 from UCB), formulation **14**, leads to further improvement of the impact strength and reactivity without detrimental effect on the other characteristics. With the acylphosphine oxide photoinitiator (formulation **15**), the polymerization reaction proceeded twice as fast, but the optical properties of the glass laminate were not as good as with the hydroxyphenyl ketone photoinitiator (Table I).

For all these systems, it is important to keep the organosilane content to at least 1% in order to ensure good adhesion to the glass substrate. In this respect, one should mention that similar performance can be obtained by using the acrylate-grafted organosol (HIGHLINK OG 101) newly developed by Hoechst. It consists of a colloidal suspension of amorphous silica particles modified at their surface by an acrylate-terminated hydrocarbon chain, which makes them compatible with organic media. Such silicon acrylate grafts can be used as reactive diluents in UV-curable resins, in particular, for coatings and adhesives applications, where they were shown to improve the properties of the cured product.<sup>17</sup>

The light stability of these UV-cured glass laminates was tested on formulation **13** in a QUV accelerated weatherometer. After 2000 h of continuous exposure at 40°C, the laminate stayed perfectly transparent and noncolored, with a yellow index value of less than 2, while the adhesive strength remained essentially unaffected. A 10-fold increase of the weathering resistance of such cross-linked polyurethane-acrylate polymers was achieved by adding to the liquid resin small amounts (1%) of a hindered

amine light stabilizer, like Tinuvin 292.<sup>18</sup> This efficient radical scavenger was shown to have no adverse effect on the cure speed, probably because the polymerization occurs in an O<sub>2</sub>-depleted medium where the active nitrooxy radical cannot be formed.

### Glass–Polycarbonate Laminates

The UV-curing technology was also applied to produce polycarbonate–glass laminates by a fast and inexpensive process. Such safety glasses should present some distinct advantages, as they are expected to exhibit on one side the strong impact resistance that is characteristic of polycarbonates (PC) and, on the other side, the chemical inertness, scratch resistance, and hardness of mineral glass.

A major difficulty was encountered in this study when we tried to use as adhesives the various UV-curable resins developed previously for the glass–glass laminates. Indeed, all the formulations containing 10% or more of AA were found to react with the PC plate, with a total loss of adhesion. Moreover, as a result of this chemical attack, such laminates rapidly lost their transparency, making them useless for safety glass applications. This detrimental effect can be suppressed by lowering the AA content, down to less than 5%. The UV-cured intercalate then shows good adhesion to the PC plate, which remains transparent, but at the same time, it loses its adherence to the mineral glass plate (Table III).

To overcome this difficulty, we first protected the surface of the PC plate in contact with the adhesive resin by a thin UV-cured coating having less than 5% AA in its formulation. Under those conditions, a resin containing 10% or more of AA was found to have good adhesion after UV-curing to both the glass plate and the coated PC plate. Such laminates are highly transparent and have excellent impact resistance. Their weak point lies in the sensitivity of PC to sunlight, moisture, and acidic pollutants, to which they will be exposed in outdoor applications. The degradation of the PC can be prevented to a large extent by sandwiching the PC plate, coated on both sides, between two glass plates (Fig. 3). These three-part laminates, glass–PC–glass, have the same chemical resistance and surface properties as those of glass–glass laminates, but they exhibit higher impact resistance due to the presence of the PC core and also because of the related thickness increase (16 mm instead of 10 mm).

It should be noted that the PC used in this study contained some light-stabilizers and that it is therefore not transparent in the near-UV where the photoinitiator absorbs. The photocuring of the acrylate

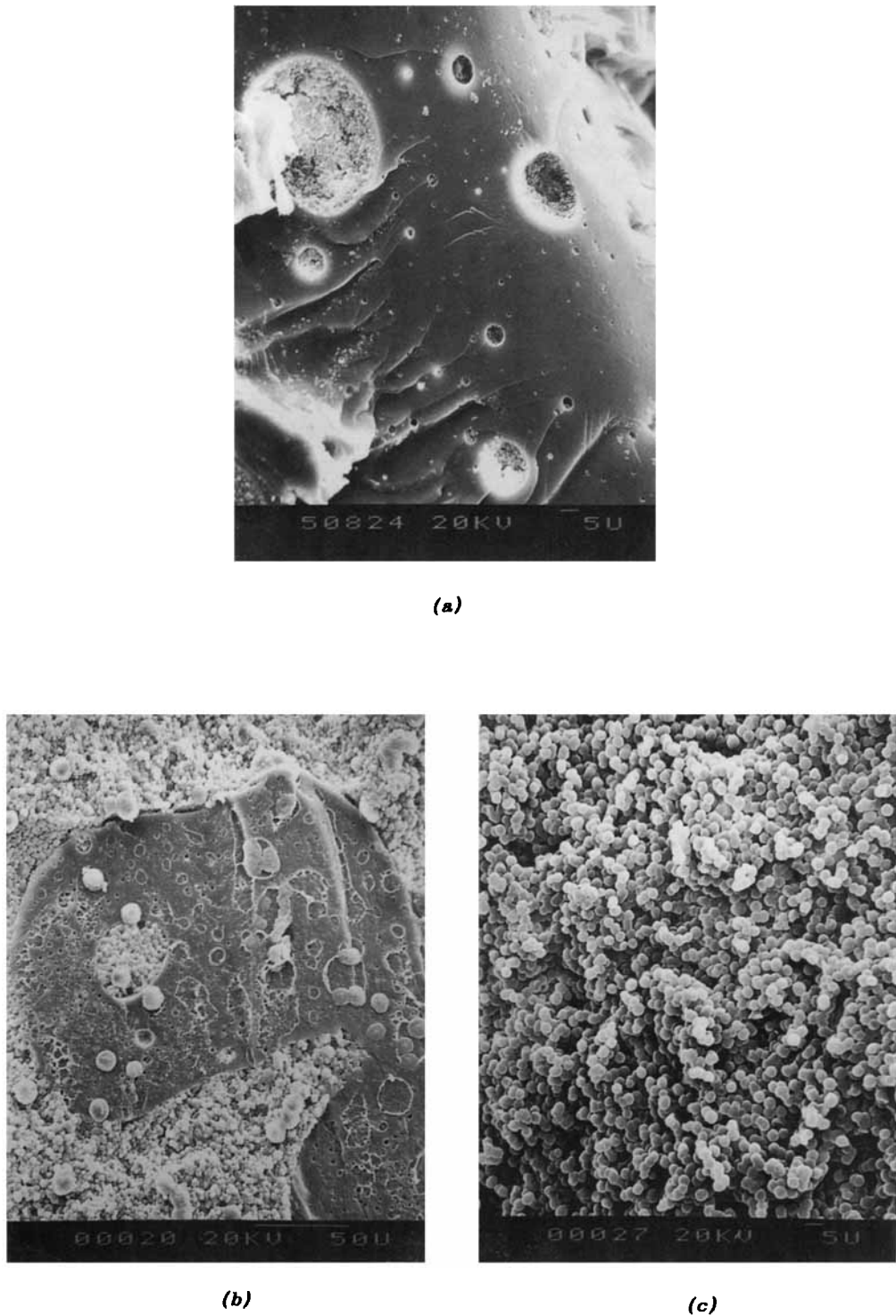


**Figure 7** SEM micrographs of the fractured surface for the 10% PMMA-containing samples at various molar ratios cured isothermally at 110°C to 45–65% conversion. (a) MR = 1/1,  $\alpha$  = 48.8%; (b) MR = 3/1,  $\alpha$  = 63.0%; and (c) MR = 6/1,  $\alpha$  = 49.7%; (a) and (c) magnify at 1000 $\times$  and (b) at 500 $\times$ .

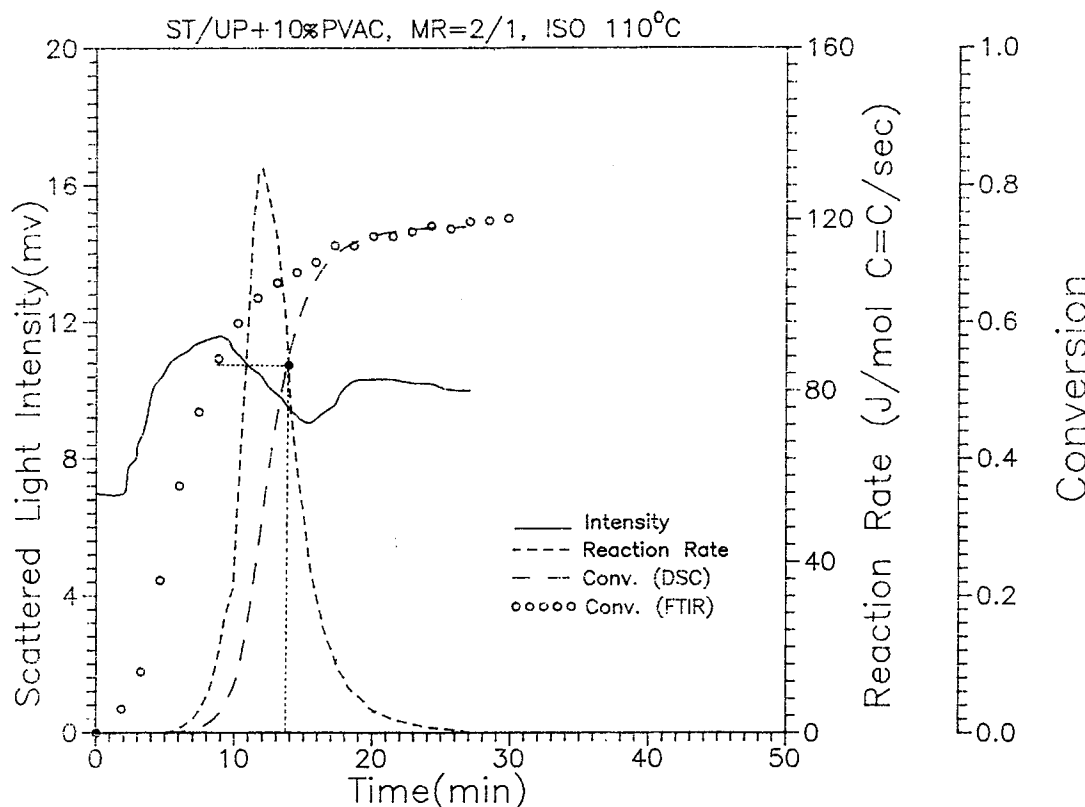


**Figure 8** Scattered light intensity vs. time profile for the 10% PVAc-containing sample with  $MR = 2/1$  cured at  $110^\circ\text{C}$ . The reaction rate and overall conversion profiles measured by DSC and the overall conversion profile measured by FTIR are also plotted for comparison. The filled circle designated in the DSC rate profile denotes the point corresponding to the maximum scattered light intensity (see text).

overlapping of primary microgel particles in that direction would not be changed. In other words, for 5–10 layers of globules (the average diameter taken as  $1\text{ }\mu\text{m}$ ) overlapped in the thickness direction of the film used, there would be at least 50–100 layers of primary microgel particles (the average diameter taken as  $0.1\text{ }\mu\text{m}$ ) closely overlapped.

In light of the comment above, the use of very thin FTIR films (also about 5–10  $\mu\text{m}$  in sample thickness) and the films in LALLS experiments would essentially make no distinction on the cure kinetics when compared with that carried out in DSC sample pan. Therefore, for the cure kinetics of UP resins, one could confidently correlate chemical information on the extent of cure by FTIR with that offered by DSC. Besides, their correlation with morphological changes observed by optical microscopy and SEM and with phase separation characteristics from LALLS results in this work could be justified.

In Figures 8 and 9, the initial value of the scattered light intensity was above zero, which could be caused by dust on the cover glasses.<sup>9</sup> It could also

be due to either the “dark current” characteristic of the detector used or the globules generated early in the reaction as observed from the corresponding photomicrographs.<sup>14</sup> For both systems, the measured intensity increased to a maximum point due to the formation of increasing number of globules, and then decreased because of the formation of microvoids and microcracks that could completely scatter the transmitted light emerging from the sample. The scattered light intensity was increased eventually to a pretty much constant value since the number of microvoids and microcracks was reduced and the number of globules generated was elevated [see Figs. 1(e) and 2(f)]. Both the globules and microvoids would finally reach constant values in numbers at the end of the reaction.

At the maximum scattered light intensity, the reaction was stopped by quenching the sample that was pasted between two microscope cover glasses into liquid nitrogen. By using an ultrasonic vibrator, the sample in the form of a film between the two cover glasses was taken out. FTIR was then used to

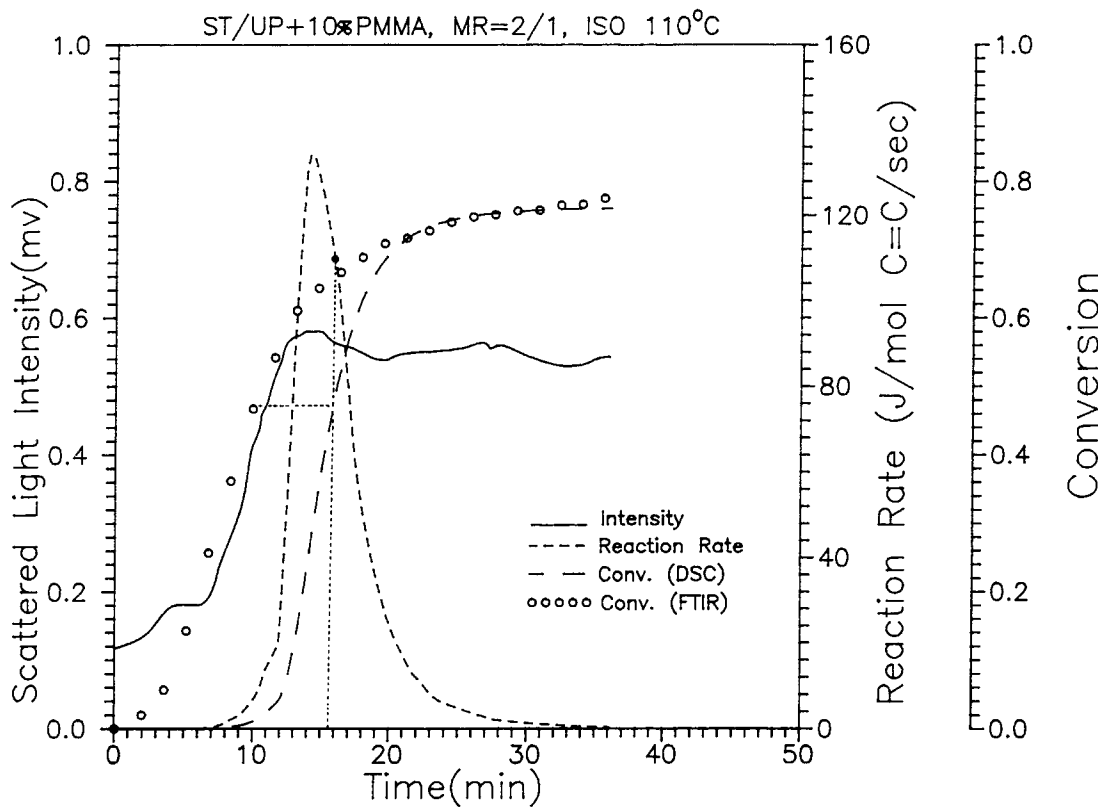


**Figure 9** Scattered light intensity vs. time profile for the 10% PMMA-containing sample with  $MR = 2/1$  cured at  $110^\circ\text{C}$ . The reaction rate and overall conversion profiles measured by DSC and the overall conversion profile measured by FTIR are also plotted for comparison. The filled circle designated in the DSC rate profile denotes the point corresponding to the maximum scattered light intensity (see text).

measure the conversions of styrene and polyester  $\text{C}=\text{C}$  bonds, where styrene loss in the FTIR measurement was also corrected. It was found that for the PVAc-containing sample,  $\alpha_S = 0.47$ ,  $\alpha_E = 0.61$ , and  $\alpha_{\text{TOT}} = 0.52$ , while for the PMMA-containing sample,  $\alpha_S = \alpha_E = \alpha_{\text{TOT}} = 0.47$ . In order to find the corresponding location in the DSC rate profile when the maximum scattered light intensity occurs, the directly measured conversion was first designated on the conversion profile measured by FTIR. Subsequently, on the same basis of the overall  $\text{C}=\text{C}$  conversion, the corresponding cure time in the DSC measurement at the maximum scattered light intensity was found. Finally, the maximum scattered light intensity was found to take place shortly after the maximum peak in the DSC profile as designated (filled circle) in Figures 8 and 9. This was also confirmed by our SEM micrographs shown in Figures 1(c)–(e) and 2(d)–(f) for both systems, where a great number of globules was generated and became more

packed around the maximum peak in the DSC rate profile, and microvoids and microcracks appeared markedly after the peak of the rate profile.

When compared with Figures 8 and 9, it is seen that the increase of the scattered light intensity at the maximum peak in reference to the initial value appeared much lower for the PMMA-containing sample than that for the PVAc-containing sample (0.5 vs. 5 mv). Also, the percentage of decrease in the scattered light intensity from the peak value to the local minimum was lower for the PMMA-containing sample (10 vs. 60%). The former was due to the fact that the globules generated were fewer in number for the PMMA-containing sample, whereas the latter was because that microvoids and microcracks generated were limited to the PMMA-dispersed phase for the PMMA-containing sample, instead of existing all over the sample in the PVAc continuous phase for the PVAc-containing sample (see Figs. 1 and 2).

## DISCUSSION

### Effects of LPA on Microgel Formation

The microgel formation is the main feature in the cure of UP resins,<sup>16,17</sup> where the styrene-unsaturated polyester copolymerization is involved. Adding LPA in the neat UP resin reaction system could enhance the microgels (i.e., globules in Figs. 1 and 2) to be clearly identified throughout the reaction. This is because a layer of LPA could cover the surface of microgel particles when the microgel particle phase separates from the matrix of unreacted resins containing LPA. The LPA would then be served as segregating agents, which could cause the much less merging of microgel particles and thus retain the identity of the individual microgel particle.

### Effects of Phase Characteristics on the Morphology

The effects of temperature, molar ratio of styrene to polyester C=C bonds, and LPA content on phase characteristics of the static ternary systems of ST-UP-PVAc and ST-UP-PMMA prior to reaction have been discussed in details in Part I of this series.<sup>12</sup> The phase diagrams at 25°C are shown in Figure 10, where the phase boundary is not enclosed since the phase equilibrium at a higher level of LPA content would not be feasible.

To facilitate our discussion, it is assumed that for the ST-UP-LPA system cured at 110°C, once the reaction-induced phase separation occurs at the early stage of the reaction, the mass transfer into or out of the continuous phase or the dispersed phase would essentially cease. Also, the compositions in either phase could be roughly represented, in an average sense, by those based on the static phase characteristics at 25°C as shown in Figure 10. This is because the increase in molecular weights of the reacting species via crosslinking reactions would enhance the phase separation in the same direction as the lowering in mixing temperature would. In reality, the true compositions of the two phases may depend on dynamic phase characteristics, which would be connected with the reaction kinetics and the rate of ongoing phase separation. It should be noted that since the phase separation would be less promoted by the effect of lowering the mixing temperature than by the effect of increasing molecular weights of the reacting species during the reaction, an immiscible two-phase mixture for the ST-UP-LPA system at 25°C after a phase equilibrium would invariably exhibit a two-phase microstructure con-

taining a continuous phase and a dispersed phase during the reaction at 110°C. The converse is not necessarily true.

As shown in Table I, in either the continuous or the dispersed phase, the resulting morphology after the cure at 110°C may exhibit a flakelike or globule microstructure, which can be judged from the molar ratio of styrene to polyester C=C bonds and the percent of LPA in the corresponding phase based on the phase characteristics at 25°C. In general, either high molar ratio or high percent of LPA could exert profound segregating effects on microgel particles and would lead to a globule microstructure. In the case of inadequate overall segregating effects on microgel particles, a flakelike microstructure or a coexistence of flakelike and globule microstructures would result. In contrast to that shown in Table I, a flakelike microstructure was found in the continuous phase for the PVAc-containing sample with 4% PVAc and at MR = 2/1 by Bucknall et al.,<sup>10</sup> which would be essentially caused by the inadequate segregating effect of LPA as explained here.

### Effect of Reaction Temperature on the Morphology

In the cure of UP resins, the segregating effect of styrene on microgel particles at high molar ratios, such as  $MR \geq 3/1$ , would be greatly enhanced by decreasing the level of reaction temperature. For example, at 30–40°C, the microgel particles could be identified on the fractured surface for the ultimately cured sample of neat UP resins with  $MR \geq 3/1$ .<sup>16,17</sup> This is because at higher molar ratios, the styrene content would exceed that needed to crosslink with polyester C=C bonds, and the surplus styrene would then rely on its homopolymerization to raise the final conversion. Since styrene homopolymerization tends to be unfavorable due to high activation energies of the reaction at such low temperatures,<sup>18</sup> therefore the local microgel particles dispersed in the unreacted resin matrix could emerge. In contrast, higher reaction temperatures could promote the intermicrogel reactions at the later stage of reaction via styrene homopolymerization or branching growth of styrene on polyester C=C bonds, resulting in the connecting of the local microgel particles as a whole and the formation of a flakelike microstructure for the neat UP resin system at high molar ratios.

For ST-UP-LPA systems, both LPA and styrene could exert the segregation effect on microgel particles. As the level of reaction temperature increases,

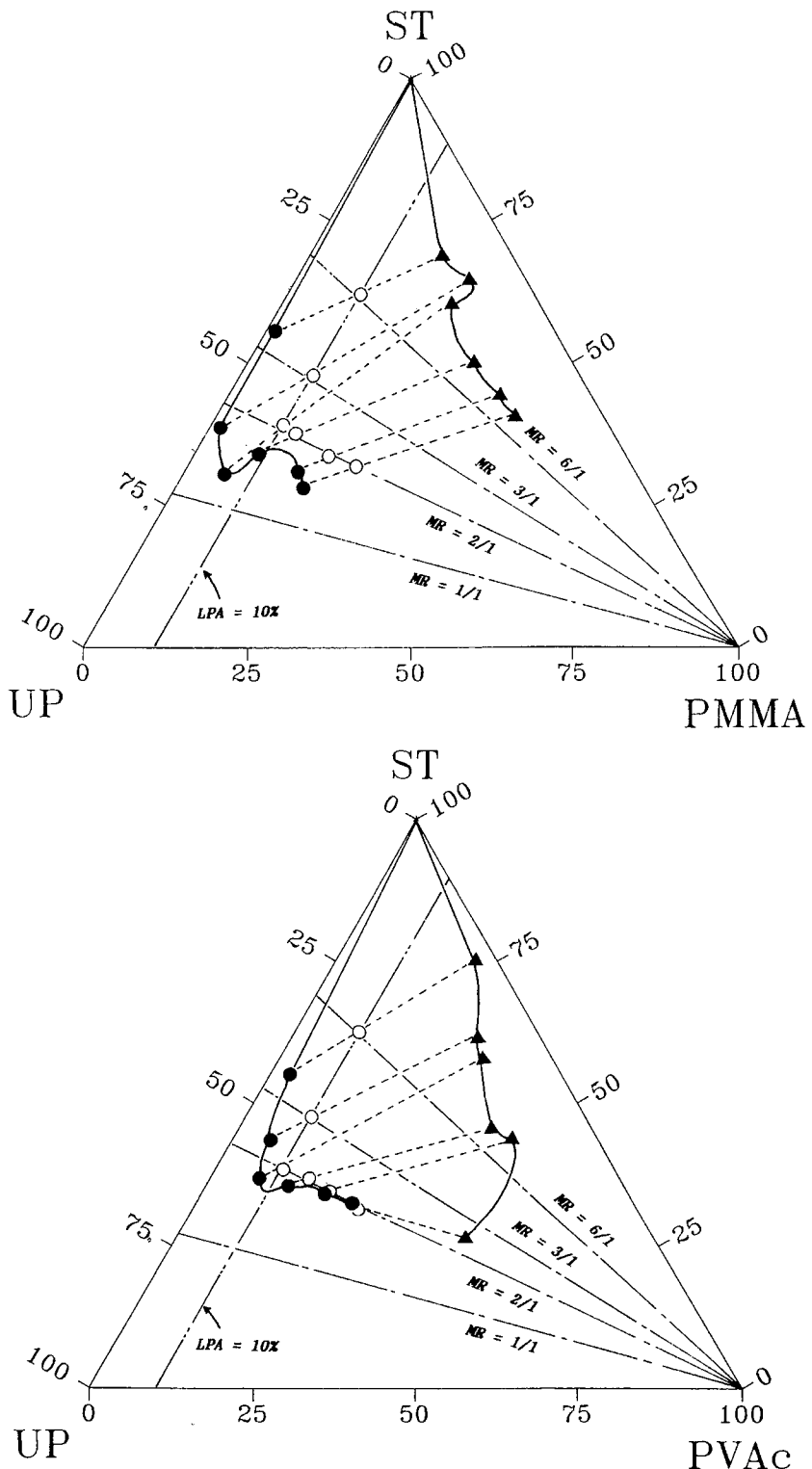


**Figure 10** Ternary phase diagrams of (a) ST-UP-PMMA, and (b) ST-UP-PVAc systems before the reaction at 25°C. The dotted tie lines connect the compositions of the continuous phase (●) and the dispersed phase (▲) in equilibrium. The composition of the whole mixture is designated as (○). Inside the phase boundary is a two-phase region, while outside the boundary a single-phase region. The constant molar ratio lines at  $MR = 1/1$ ,  $2/1$ ,  $3/1$ , and  $6/1$  and the constant LPA line at 10% are also shown.

**Table I** Resulting Microstructure after the Cure at 110°C for the ST-UP-PMMA and ST-UP-PVAc Systems with 10% by wt. of LPA and at MR = 2/1, 3/1, and 6/1

Molar Ratio	ST-UP-PMMA System		ST-UP-PVAc System	
	Dispersed Phase	Continuous Phase	Dispersed Phase	Continuous Phase
MR = 2/1	Globule (good) <sup>a</sup>	Flakelike (poor)	Globule (good)	Globule (good)
MR = 3/1	Globule (good)	Flakelike + Globule (fair)	Globule (good)	Globule (good)
MR = 6/1	Globule (good)	Globule (good)	Globule (good)	Globule (good)

<sup>a</sup> The evaluation of overall segregating effects of LPA and styrene on microgel particles as evidenced by the resulting microstructure after the cure (see text).

the amount of LPA needed to achieve the same extent of segregation on microgel particles would then be larger due to a concomitant decrease of the styrene segregating effect on microgel particles as mentioned above. For example, at the PVAc concentration of 3–15%, the individual globule could be observed throughout the sample for the UP resin with MR = 2/1 cured at 80°C.<sup>11</sup> In contrast, for the observation of the similar globule microstructure, 10% and 8–16% of the PVAc concentration should be employed for the UP reaction system cured at 110°C in this study and at 130°C,<sup>5</sup> respectively. The exact concentration of PVAc may also depend on its chemical nature and molecular weight.<sup>10</sup>

### Effects of LPA on Volume Shrinkage Control

Figure 10 shows that for both ST-UP-PMMA and ST-UP-PVAc systems at 25°C, as the amount of LPA increases, the percent of LPA content in either the continuous phase or the dispersed phase also increases. In the cure of UP resins with higher content of LPA, the formation of clearly identified microgel particles could then be greatly enhanced, and the volume shrinkage control would be better. This is because the microcracks and microvoids for relieving molded parts of the shrinkage strain due to polymerization would be generated only in the phase region that contains clearly identified microgel particles, rather than in the phase region characterized by a flakelike microstructure. Therefore, in the cure of low-shrink UP resins, the increase of the scattered light intensity at the maximum peak in reference to the initial value, which depends on the concentration of clearly identified microgel particles generated, and the percentage of decrease in the scattered light intensity from the peak value to the local minimum, which depends on the concentration of microvoids and microcracks generated, as shown in Figures 8

and 9 could possibly be employed as two index parameters for the performance of volume shrinkage control. In general, the larger the two index parameters, the better the volume shrinkage control would be. Indeed, it is well known that PVAc provides a better volume shrinkage control than PMMA,<sup>6</sup> and the experimental results of scattered light intensity in Figures 8 and 9 indicate that both of the two index parameters are larger for the PVAc-containing sample than for the PMMA-containing sample. However, since the light-scattering method employed here is not rigorous, further work needs to be done to verify the interrelationships between the shrinkage control and the index parameters from the light-scattering results.

### CONCLUSIONS

The effects of LPA on the morphological changes and the phase separation for the UP resins at various molar ratios of styrene to polyester C=C bonds have been investigated at 110°C. Adding LPA in the neat UP resin reaction system could enhance the microgel particles to be clearly identified throughout the reaction. This is because a layer of LPA could cover the surface of microgel particles when the microgel particle phase separates from the matrix of unreacted resins containing LPA. The segregating effect of LPA would cause the much less merging of microgel particles and thus retain the identity of the individual microgel particle. For the ST-UP-LPA system, the static phase characteristics at room temperature could be employed as a rough guide for accounting for the observed morphology during the reaction at 110°C.

This work was sponsored by the National Science Council of the Republic of China (NSC 81-0405-E-011-13). Material donation from Eternal Chemical Corporation, Taiwan, is also greatly appreciated.

## REFERENCES

1. E. J. Bartkus and C. H. Kroekel, *Appl. Polym. Symp.*, **15**, 113 (1970).
2. V. A. Pattison, R. R. Hindersinn, and W. T. Schwartz, *J. Appl. Polym. Sci.*, **18**, 2763 (1974).
3. A. Siegmann, M. Narkis, J. Kost, and A. T. Dibenedetto, *Int. J. Polym. Sci.*, **6**, 217 (1978).
4. V. A. Pattison, R. R. Hindersinn, and W. T. Schwartz, *J. Appl. Polym. Sci.*, **19**, 3045 (1975).
5. C. B. Bucknall, P. Davis, and I. K. Partridge, *Polymer*, **26**, 108 (1985).
6. K. E. Atkins, in *Polymer Blend*, Vol. 2, D. R. Paul and S. Newman, Eds., Academic Press, New York, 1978, Chap. 23.
7. L. Kiaee, Y. S. Yang, and L. J. Lee, *AIChE Symp. Series*, **84**, 52 (1988).
8. C. P. Hsu and L. J. Lee, *Plast. Eng.*, November, 45 (1989).
9. L. Suspene, D. Fourquier, and Y. S. Yang, *Polymer*, **32**, 1593 (1991).
10. C. B. Bucknall, I. K. Partridge, and M. J. Phillips, *Polymer*, **32**, 786 (1991).
11. C. P. Hsu, M. Kinkelaar, P. Hu, and L. J. Lee, *Polym. Eng. Sci.*, **31**, 1450 (1991).
12. Y. J. Huang and C. C. Su, *J. Appl. Polym. Sci.*, to appear.
13. Y. J. Huang, T. J. Lu, and W. Hwu, *Polym. Eng. Sci.*, **33**, 1 (1993).
14. C. C. Su, M. S. Thesis, National Taiwan Institute of Technology, 1992.
15. E. J. Melby and J. M. Castro, in *Comprehensive Polymer Science*, Vol. 7, S. G. Allen, J. C. Bevington, and S. L. Aggarwal, Eds., Pergamon Press, New York, 1989, p. 71.
16. C. P. Hsu and L. J. Lee, *Polymer*, **32**, 2263 (1991).
17. Y. S. Yang and L. J. Lee, *Polymer*, **29**, 1793 (1988).
18. Y. J. Huang and C. J. Chen, *J. Appl. Polym. Sci.*, **46**, 1573 (1992).

Received March 22, 1994

Accepted June 23, 1994